analytical chemistry

pubs.acs.org/ac Article

Ag^+ Ion Binding to Human Metallothionein-2A Is Cooperative and Domain Specific

Shiyu Dong, Mehdi Shirzadeh, Liqi Fan, Arthur Laganowsky, and David H. Russell*

Cite This: *Anal. Chem.* 2020, 92, 8923−8932 Read Online

ACCESS | Metrics & More | Article Recommendations | Supporting Information

ABSTRACT: Metallothioneins (MTs) constitute a family of cysteine-rich proteins that play key biological roles for a wide range of metal ions, but unlike many other metalloproteins, the structures of apo- and partially metalated MTs are not well understood. Here, we combine nano-electrospray ionization-mass spectrometry (ESI-MS) and nano-ESI-ion mobility (IM)-MS with collision-induced unfolding (CIU), chemical labeling using *N*-ethylmaleimide (NEM), and both bottom-up and top-down proteomics in an effort to better understand the metal binding sites of the partially metalated forms of human MT-2A, viz., Ag_4-MT. The results for Ag_4-MT are then compared to similar results obtained for Cd_4-MT. The results show that Ag_4-MT is a cooperative product, and data from top-down and bottom-up proteomics mass spectrometry analysis combined with NEM labeling revealed that all four Ag^+ ions of Ag_4-MT are bound to the β-domain. The binding sites are identified as Cys13, Cys15, Cys19, Cys21, Cys24, and Cys26. While both Ag^+ and Cd^{2+} react with MT to yield cooperative products, i.e., Ag_4-MT and Cd_4-MT, these products are very different; Ag^+ ions of Ag_4-MT are located in the β-domain, whereas Cd^{2+} ions of Cd_4-MT are located in the α-domain. Ag_6-MT has been reported to be fully metalated in the β-domain, but our data suggest the two additional Ag^+ ions are more weakly bound than are the other four. Higher order Ag_i-MT complexes (i = 7−17) are formed in solutions that contain excess Ag^+ ions, and these are assumed to be bound to the α-domain or shared between the two domains. Interestingly, the excess Ag^+ ions are displaced upon addition of NEM to this solution to yield predominantly Ag_4NEM_{14}-MT. Results from CIU suggest that Ag_i-MT complexes are structurally more ordered and that the energy required to unfold these complexes increases as the number of coordinated Ag^+ increases.

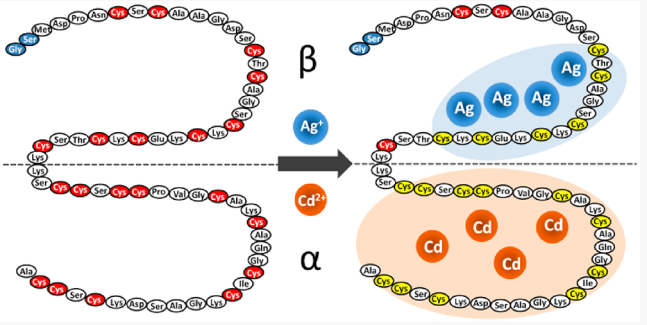

Metallothioneins (MTs) constitute a family of cysteine-rich small proteins that bind a wide range of metal ions.[1−3] While the exact biological function(s) of MTs are not fully understood, they have been implicated in diseases such as Alzheimer's, Parkinson's, and cancer, which suggests that MTs have functions other than being "sponges" for metal homeostasis, heavy metal detoxification, and antioxidation.[1,4−8] Studies of structure/function relationships of MTs are complicated by the fact that the physiologically dominant forms of MTs are the apo and partially metalated forms,[9−12] but their low abundances and conformational heterogeneity have limited the in vitro studies of partially metalated MTs using traditional structural approaches, viz., X-ray cryptography or NMR spectroscopy.[1] Apo-MTs lack well-defined tertiary structure, and structure(s) and folding stabilities of metalated species are largely determined by metal−thiolate bonds.[1,13] Structural characterization of metalated MTs has proved challenging, owing to difficulties associated with growing high-quality crystals required for X-ray crystallography. It has been equally difficult to locate metal bound cysteine residues using conventional protein NMR spectroscopy.[1,2] While it is possible to substitute NMR silent metal ions with NMR active nuclei, i.e., Zn^{2+} by $^{111}Cd^{2+}$ or $^{113}Cd^{2+}$[13] and Cu^+ by $^{109}Ag^+$,[14] it is unclear that such replacements are isostructural.[1] There is strong evidence that binding of MTs involves two domains and that Cd^{2+} and Zn^{2+} form M_4Cys_{11} clusters in the α-domain and M_3Cys_9 clusters in the β-domain.[1,13,15,16] Both Cd^{2+} and Zn^{2+} adopt tetrahedral coordination spheres with each metal ion coordinated to four thiolates; however, the coordination of monovalent metal ions, i.e., Ag^+ and Cu^+, is more likely to involve digonal and/or trigonal geometries.[17,18] The redox-stable monovalent Ag^+ was previously used to model redox-active Cu^+−MT complexes;[14,17,19] however, Ag-MT and Cu-MT differ significantly in terms of metalation and binding geometries.[19] For example, Scheller et al.[20] reported that up to 20 Cu^+ ions bind to MT, whereas Zelazowski[21] and

Received: February 24, 2020
Accepted: June 9, 2020
Published: June 9, 2020

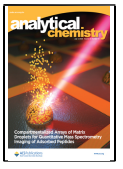

https://dx.doi.org/10.1021/acs.analchem.0c00829
Anal. Chem. 2020, 92, 8923−8932

Scheuhammer and Cherian[22] reported that 17−18 Ag^+ ions bind to MT. The structures for Cu-MT and Ag-MT complexes from *Saccharomyces cerevisiae* have been reported by Bertini et al.[23] and Narula et al.[14] Both Cu^+ and Ag^+ adopt mixed trigonal planar and linear/digonal coordination; however, the reported structures are not identical.[23] X-ray absorption spectroscopy has been used to study the binding geometries of Cu^+ and Ag^+ for mammalian MT; Cu^+ is more likely to adopt trigonal geometry, while Ag^+ is reported to occupy trigonal and digonal coordination.[24,25]

In recent years, there has been growing interest in using mass spectrometry for studies of metalloproteins. Fenselau and co-workers were one of the first to employ electrospray ionization-mass spectrometry (ESI-MS) for studies of MTs.[26,27] Increasing numbers of investigators have incorporated ESI-MS in their studies. Kagi and Vallee reported one of the earliest attempts to isolate MT from equine renal cortex,[28] and Kagi and co-workers have reported important applications of both NMR[13,29,30] and MS[31] for studies of structure of Cd_7-MT and cooperativity of metalation. Lobinski and co-workers used both microscale purification techniques (HPLC, capillary electrochromatography) and trace analysis techniques, including ESI-MS, to successfully detect MT isoforms from different systems.[32−34] Atrian, Capdevila, and co-workers used ESI-MS to investigate metal binding of MT from different species and to bridge the gap between phytochelatins and metallothions.[35−38] Stillman and co-workers have made extensive use of ESI-MS for studies of ion reactivity and kinetics in metalation reactions of MT employing a broad range of metal ions.[39−41] Blindauer and co-workers have reported MT expression in different species and dynamics of metal binding and release employing multiple analytical methods including MS.[42−44]

While ESI-MS is able to distinguish different metalated species on the basis of mass-to-charge ratios, the mass spectra do not provide information related to metal ion binding sites, structural changes that accompany metal ion binding, or stabilities of the metal−MT complexes. Here, a comprehensive strategy employing both ESI mass spectrometry and ESI ion mobility-mass spectrometry (IM-MS) is used to investigate Ag^+ binding to human MT-2A (denoted as MT). The major products formed upon addition of Ag^+ to MT are Ag_i-MT (i = 4−17). The results presented provide clear evidence that the cooperative binding product, viz., Ag_4-MT, is formed by domain-specific metal ion binding to the β-domain, unlike the similar cooperative binding product, Cd_4-MT, which is formed by the addition of Cd^{2+} to the α-domain.[45] Additional evidence for domain specific binding for Ag^+ and Cd^{2+} to MT is obtained by mixed metalation reactions.[46] The combination of nano-ESI and IM-MS affords direct measurements of the ion shape/size as well as conformational diversity of the ion population,[47−50] which can be compared to conformational preferences of apo- and partially metalated MT.[45,46,51−53] Prior studies have shown that, under suitable instrumental conditions, it is possible to maintain noncovalent interactions as well as metal−ligand interactions formed in MTs.[46,51,54] Proteomics strategies, including "bottom-up" and "top-down", are used in concert with *N*-ethylmaleimide (NEM) labeling to ascertain the domain specific metalation that yields Ag_4-MT.[1,19,55,56] IM-MS is also used to perform collision-induced unfolding (CIU) experiments on Ag_4-MT as well as the higher metalated species Ag_i-MT (i = 5−17), which provide information for the relative stabilities of the gas-phase ions.[48,49,57−62]

EXPERIMENTAL SECTION

Silver acetate, cadmium acetate, ammonium acetate, zinc acetate, diethylenetriaminepentaacetic acid (DTPA), dithiothreitol (DTT), tris (2-carboxyethyl) phosphine hydrochloride (TCEP), and *N*-ethylmaleimide (NEM) were purchased from Sigma-Aldrich (St. Louis, MO). Sequencing grade modified trypsin was purchased from Thermo Fisher Scientific (Waltham, MA). Deionized water (18.2 MΩ) was obtained from a Milli-Q water apparatus (Millipore, Billerica, MA). Micro Bio-Spin 6 columns were purchased from Bio-Rad Laboratories, Inc. (Hercules, CA). Details for MT expression and purification, Zn_7-MT demetalation, and in solution digestion for bottom-up proteomics are included in the Supporting Information.

The Ag^+ metalation experiment was performed by sequential addition of 1.75 μL of 1 mM (1:1 molar ratio of Ag^+/apo-MT, denoted as one equivalent) silver acetate to 100 μL of MT solution until the metalation degree of products showed saturation.[45] After each Ag^+ addition, the solution was incubated at room temperature for 1 h and then analyzed by nESI-MS. All experiments were performed on a Waters Synapt-G2 HDMS instrument (Manchester, UK). Instrumental conditions were tuned to minimize collisional heating as previously described.[52] All ESI-MS experiments were carried out using nano-ESI capillaries (pulled borasilicate emitter tips ranging in size (IDs ∼ 5−10 μm), which provide more reproducible mass spectra containing much less background noise.

A Ag/Cd mixture solution was prepared by mixing 1 mM silver acetate and 1 mM cadmium acetate solution in 1:1 ratio. Apo-MT was mixed with 7 equiv of the Ag/Cd mixture and incubated at room temperature for 1 h before analysis. The Ag/Cd mixed metal synthesis experiment was performed by adding ∼3.5 equiv of 1 mM Ag^+ to apo-MT and incubating for 1 h at room temperature. Afterward, 3.5 equiv of 1 mM Cd^{2+} was added, and the sample was incubated for 1 h at room temperature. Mass spectra and CIU heat maps of the product ions were obtained. A similar set of experiments, which involved switching the order of the addition of Ag^+ and Cd^{2+}, was performed.

Ag_4-MT was obtained by metalation of apo-MT (adding 7 μL of 1 mM Ag^+ to a 17.5 μM apo-MT solution). Four μL of 10 mM NEM was added to Ag_4-MT and incubated for 1 h at room temperature to completely react with metal-free cysteinyl groups. The alkylated metalated products (Ag_4NEM_{14}-MT) were mass-selected for direct sequencing by tandem mass spectrometry (top-down approach). The approach used to characterize metal binding sites is a combination of MS, CID, IM, and MS, denoted as MS-CID-IM-MS.[45,63−65] In this approach, CID fragment ions are dispersed in two dimensions, size-to-charge (IM) and mass-to-charge (MS). Fragment ions of different charge states fall along different trend lines in the resulting 2D spectra, which reduces spectra congestion and simplifies identification of the fragment ions.

nESI-CIU-MS experiments were carried out as described previously.[46,50] Different collision voltages were applied by changing the voltage drop (increments of 5 V) between the exit of the quadrupole and the entrance to the TWIG-trap; thus, collision energy is reported as lab-frame collision energy (E_{lab}).[46,54] Ion mobility profiles under different activation

https://dx.doi.org/10.1021/acs.analchem.0c00829
Anal. Chem. 2020, 92, 8923−8932

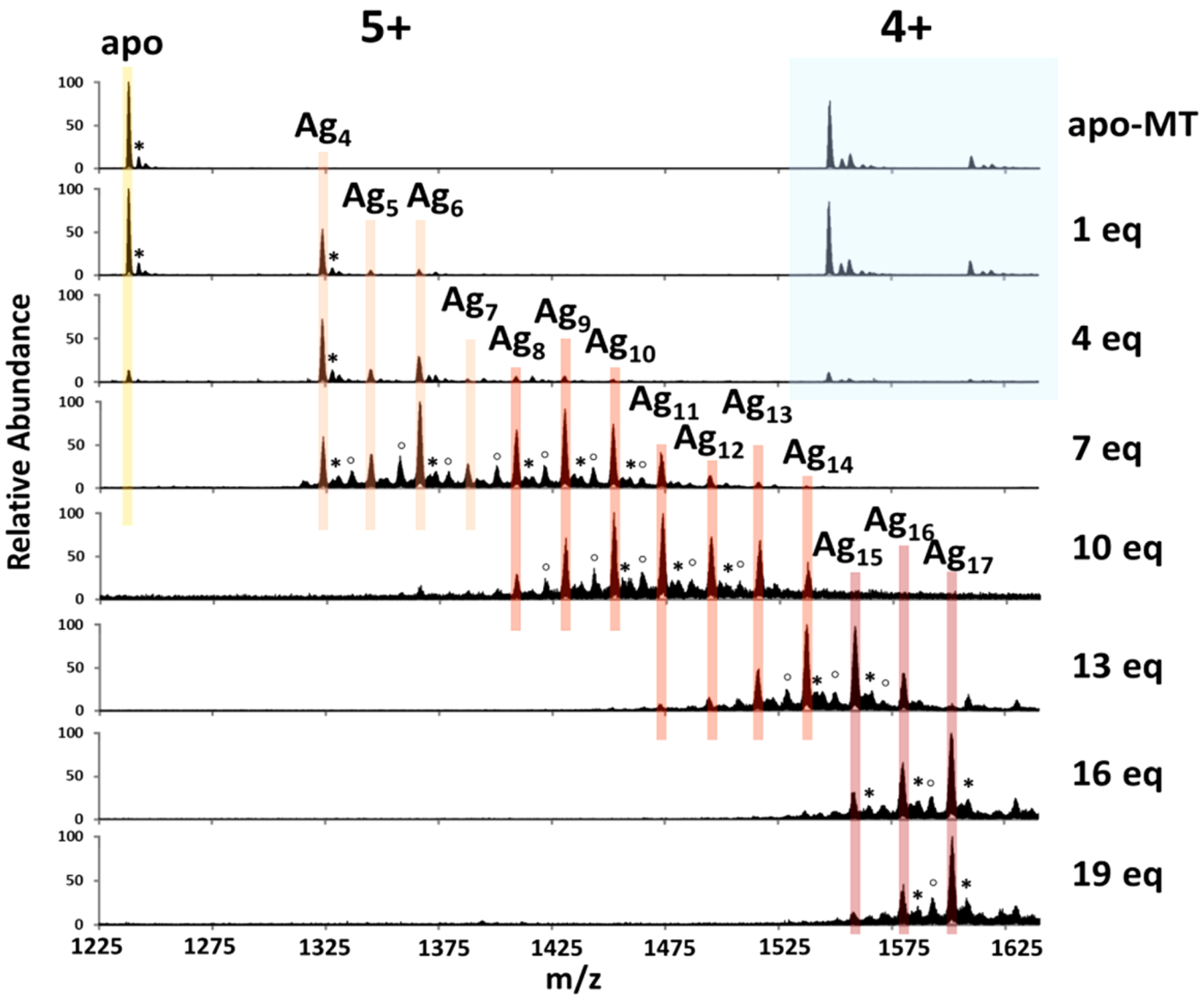

Figure 1. ESI-MS spectra taken following sequential addition of Ag^+ to apo-MT solution. Peaks with asterisks (*) and circles (○) are for ions that shifted by ~23 and ~60 Da, corresponding to sodium and acetate adducts, respectively.

energy were compiled into CIU heat maps using CIUSuite as described by Ruotolo and co-workers.[66] CIU50 data were extracted with CIUSuite2 to compare the unfolding energy.[67] Averages and standard deviations were calculated using three acquisitions. The standard deviations are within 3%.

RESULTS AND DISCUSSION

Previous studies have illustrated the utility of nESI-MS and IMS for studies of MT.[1,45,51−53] nESI-MS allows detection and separation of each partially metalated MT species, while IMS provides information on the shape and size of each of partially and higher order metalated MT.[46] The integrated IM-MS experiments combined with covalent chemical labeling with NEM, top-down and bottom-up proteomics with MS-CID-IM-MS, and collision-induced unfolding (CIU) are designed to better assign metal ion binding site, structure, and stabilities of products formed by reactions of Ag^+ with MT. Rotationally averaged collision cross section (CCS) profiles obtained by ion mobility for the 5^+ apo-MT ions are multicomponent, a signature for a conformational heterogeneity, whereas those for 4^+ apo-MT ions are narrow, indicative of an ion population that contains less conformational diversity.[68,69] Owing to differences in the conformational diversities of the ion population, the following sections are focused exclusively on the metalation reactions of the MT^{5+} ions. It should be noted however that the rates of reactions and the number of metal ions added to MT are similar for both charge states.

Synthesis of Human Ag_i-MT Complexes. Titration can be used to measure the kinetics of the metalation reactions, thereby identifying cooperative binding behavior.[3] Figure 1 contains mass spectra acquired from Ag^+ ion titration of human MT. Although the spectral congestion that arises from the formation of adduct ions (e.g., Na^+, acetate ions, and oxidized MT) and the metalated (Ag_i-MT^{5+}) product ions complicate accurate kinetic measurements, the combined use of IMS and high mass resolution is sufficient to allow for high confidence level assignment of the product ions.[63,64,70] With increasing concentration of Ag^+ in MT solution, the abundances and numbers of metalated product ions increased. Upon addition of solutions containing Ag^+ ions, low abundance signals corresponding to Ag_i-MT (i = 1−3) and much higher abundance ions corresponding to Ag_4-MT are

https://dx.doi.org/10.1021/acs.analchem.0c00829
Anal. Chem. 2020, 92, 8923−8932

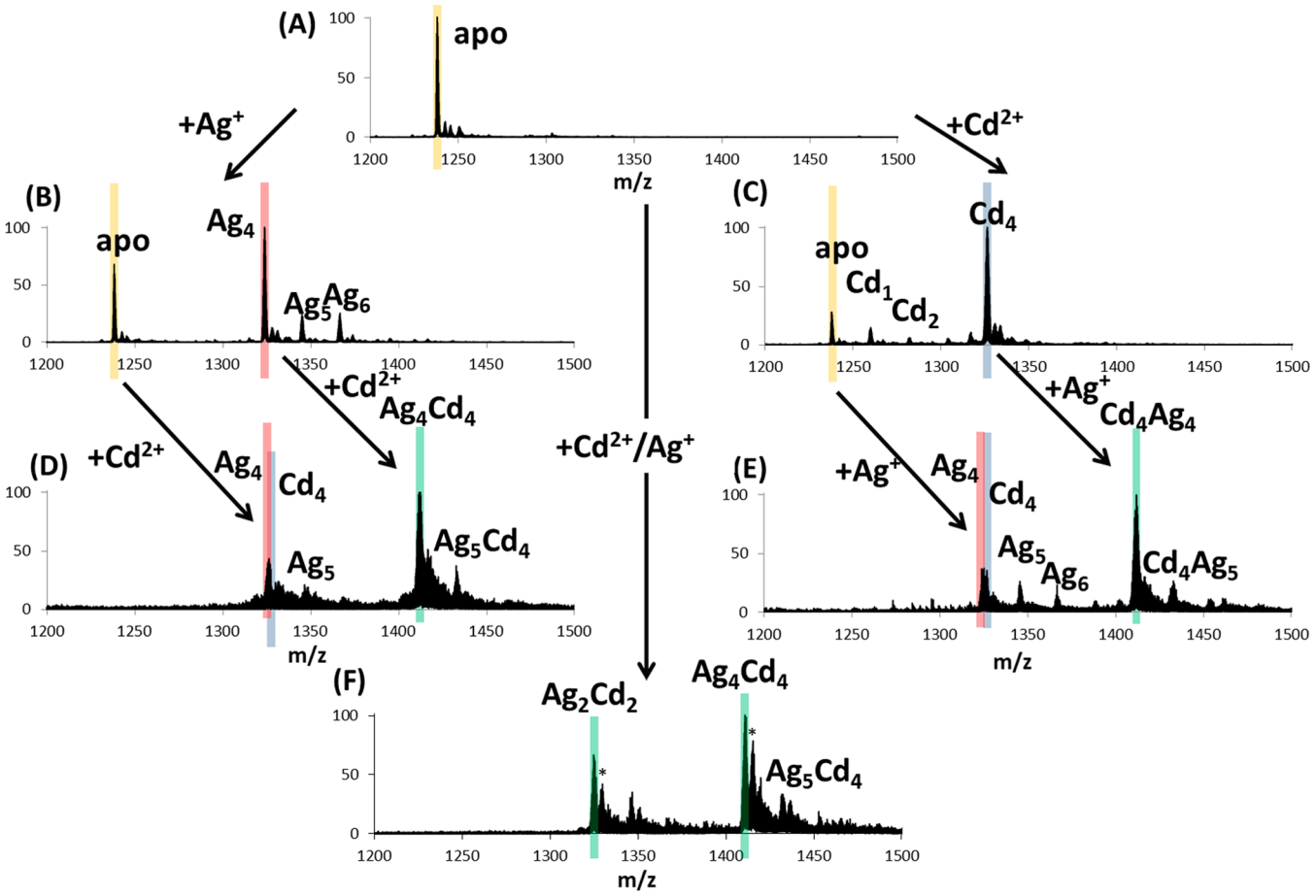

Figure 2. Mass spectra of MT obtained following the addition of Cd^{2+}/Ag^{+} ions. (A) apo-MT; (B) after addition of four equiv Ag^{+}; (C) after addition of four equiv Cd^{2+}; (D) addition of four equiv Cd^{2+} to a solution of Ag_i-MT; (E) addition of four equiv Ag^{+} to a solution of Cd_i-MT; (F) apo-MT reacted with a Ag^{+}/Cd^{2+} mixture. Peaks with an asterisk (*) are for Na^{+} adducts. The peaks in (D) and (E) labeled in red can be assigned as Ag_4-MT. The peaks labeled in blue can be assigned as Cd_4-MT. Ag_2Cd_2-MT in (F) is assigned as one MT binding two Ag^{+} and two Cd^{2+}. The identification is limited by the resolution of the instrument. A zoomed-in isotopic distribution is shown in Figure S2.

detected. The low abundance of Ag_i-MT (i = 1−3) is not surprising owing to the high concentrations of thiol ligands (20 SH group per MT molecule) as well as a high degree of cooperativity for the formation of the Ag_4-MT product ion. Similarly, the abundance of the i = 5 complex is low while that for i = 6 is relatively high. A progression of larger complexes is formed up to i = 17. It appears that the maximum number of Ag^{+} ions that can bind to MT is different when using different experimental approaches.[19,21,22,71] Zelazowski et al.[21] used circular dichroism and luminescence spectra while Scheuhammer and Cherian[22] developed a Ag saturation assay to study Ag binding, and they all reported values similar to those reported here.

Ag^{+} Displacement by a Reaction with *N*-Ethylmaleimide (NEM). NEM displacement studies were performed on the Ag_i-MT (i = 9−14) (see Figure S1). The addition of ∼20 equiv of NEM to a solution containing Ag_i-MT (i = 9−14) yielded high abundances of Ag_4NEM_{14}-MT. The results for the displacement of Ag^{+} by NEM provide additional evidence of the uniqueness of the Ag_4NEM_{14}-MT complex; specifically, the Ag^{+} ions of the Ag_i-MT (i = 9−14) complexes are considerably more labile than are those of the Ag_4-MT in solution phase.

Chen and Russell previously showed that displacement of Cd^{2+} from Cd_7-MT^{5+} by NEM occurred by a two-component, cooperative mechanism, viz., rapid displacement of three Cd^{2+} ions followed by the slow loss of the remaining four Cd^{2+} ions;[53] however, Shaw et al. reported Cd^{2+} displacement by NEM is noncooperative based on the diminished NMR signal for both the α- and β-domains.[72] Additional experimental results revealed that displacement of Cd^{2+} by NEM was domain specific; the three Cd^{2+} ions that are displaced first are from the β-domain, whereas subsequent Cd^{2+} displacement is from the α-domain.[53] Ag_4-MT is stable in NEM displacement, which further illustrates the uniqueness of its structure.

Synthesis and Stabilities of Mixed Metal (Ag^{+}/Cd^{2+}) MT: Preferred Binding Domains for Ag^{+} and Cd^{2+}. The high abundance of Ag_4-MT product ions formed by titration of MT with Ag^{+} ions is strikingly similar to that for titration of MT with Cd^{2+} ions;[51] viz., Ag_4-MT appears to be formed cooperatively. This observation raises these questions: (i) does Ag_4-MT form a stable complex that is similar to Cd_4-MT or (ii) is this product domain specific? Our previous CID results of Ag_4-MT are interpreted as evidence that most of the fragmentations result in metal-containing y-type fragment ions and metal-free b-type fragment ions, which shows that four Ag^{+} ions are more strongly interacting with cysteines in the α-domain or are located in a region between two domains.[46] However, the CID results do not preclude the possibility that metal ions migrate to new binding sites prior to dissociation. In

https://dx.doi.org/10.1021/acs.analchem.0c00829
Anal. Chem. 2020, 92, 8923−8932

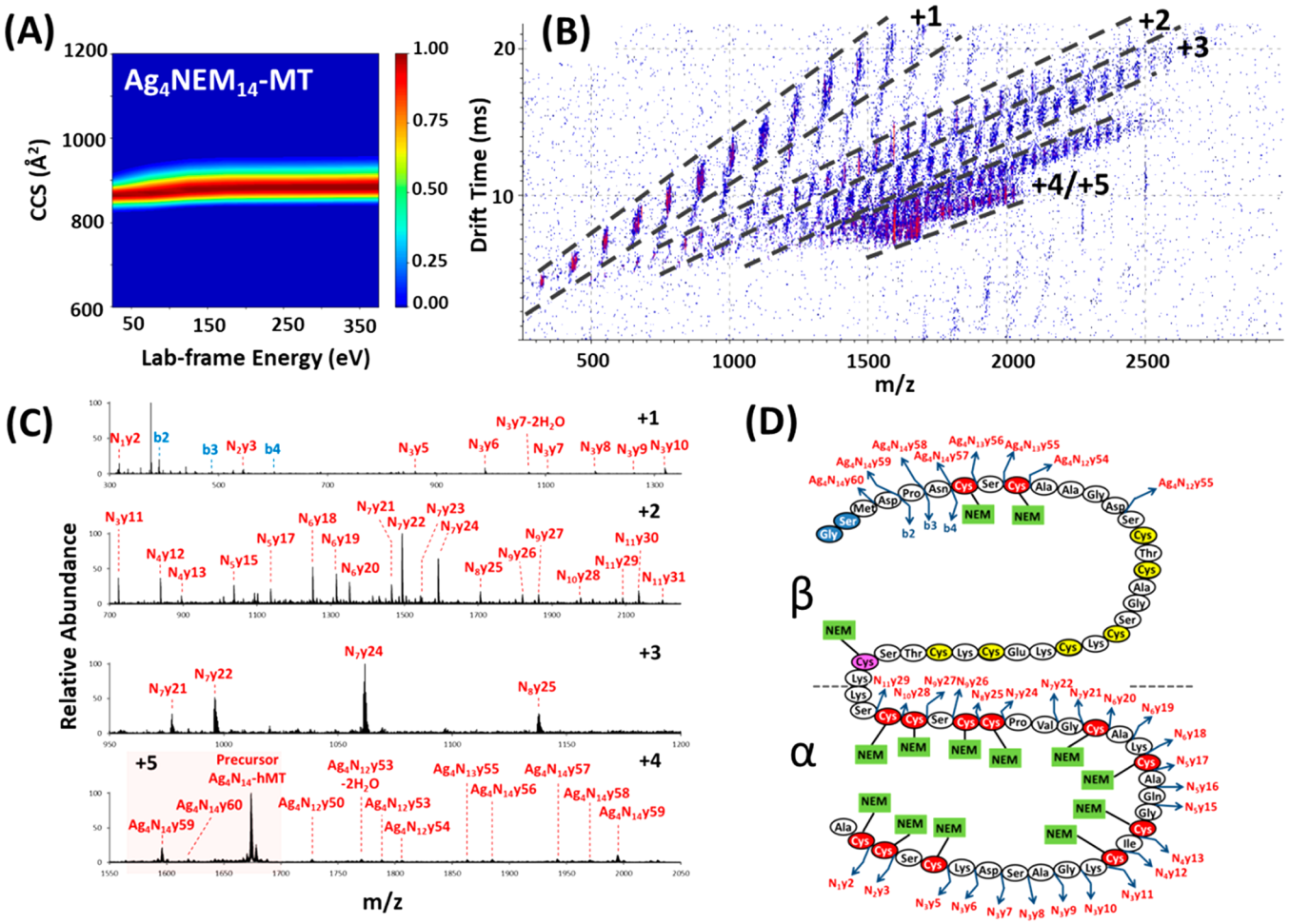

Figure 3. (A) CIU of Ag_4NEM_{14}-MT. Due to the limited fragmentation coverage from Ser12 to Ser32, 13 (colored in red) out of the 14 NEM labeled cysteines can be located with the top-down approach. Cys29 (colored in pink) is proved to be NEM labeled later with the bottom-up approach. (B) 2D MS-CID-IM-MS spectrum of Ag_4NEM_{14}-MT. The trend lines are shown for ions of different charge states as labeled (+1 to +5). (C) Extracted mass spectra for each trend line; for simplicity, NEM is abbreviated as "N". (D) Summary of the identified fragment ions and corresponding model from panel C. The labels α and β indicate the location of the domains. The N-terminal GlySer-tag, a product of tag cleavage using the TEV protease, is not included in the amino acid position assignments.

an effort to better understand the location of Ag_4-MT, cross metalation experiments were performed. These experiments were carried out by the addition of Ag^+ or Cd^{2+} to aliquots of solutions containing MT (Figure 2A) to form Ag_4-MT (Figure 2B) and Cd_4-MT (Figure 2C), respectively. Following a short incubation period (1 h), Cd^{2+} (Figure 2D) or Ag^+ (Figure 2E) was added to each solution. The final products of these reactions produced mixed metal complexes of Ag_4Cd_4-MT or Cd_4Ag_4-MT and low abundances of Ag_5Cd_4-MT or Cd_4Ag_5-MT, respectively. The Ag_4Cd_4-MT product was also formed by the addition of solutions containing equal concentrations of Ag^+ and Cd^{2+} ions to a solution of MT (Figure 2F); thus, it appears that the formation of metalated products is independent of the order of metal addition. No metal replacement is observed.

Top-Down and Bottom-Up Proteomics Following Covalent Labeling of Ag_4-MT with NEM: Where Are the Ag^+ Ions Bound? Top-down proteomics sequencing strategies were combined with NEM labeling to further characterize Ag_4-MT. The addition of excess NEM to a solution containing Ag_4-MT (see Experimental Section) yielded Ag_4NEM_{14}-MT. The formation of this product suggests that, among the 20 cysteine residues in MT, 14 are labeled by NEM and the remaining 6 are coordinated to Ag^+ ions. CIU heat maps for Ag_4NEM_{14}-MT are shown in Figure 3A. The shifts in the CCS obtained by CIU are used to track the unfolding transition of the Ag_4NEM_{14}-MT ions. The CCS of Ag_4NEM_{14}-MT is shifted from ~860 to ~880 Å^2 with collisional activation, but at higher collision energies (CEs), the CCS remains constant, indicating that the Ag_4NEM_{14}-MT complex resists unfolding. This result suggests that Ag_4NEM_{14}-MT is quite stable in the gas phase.

The $[Ag_4NEM_{14}\text{-MT}]^{5+}$ ions were also analyzed by MS-CID-IM-MS (see the Experimental Section). Mass-selected $[Ag_4NEM_{14}\text{-MT}]^{5+}$ ions are activated by energetic collisions with a neutral gas atom (Ar), and the product ions formed are then analyzed by ion mobility (on the basis of size-to-charge) and mass spectrometry (on the basis of mass-to-charge) as illustrated in Figure 3B. The mass spectra shown in Figure 3C were obtained by extracting the ion signals bracketed by the dashed lines (marked with charge states) in Figure 3B. The fragment ions in each spectrum shown in Figure 3C are then used to assign the locations of the Ag^+ ions and NEM labels.

The most abundant CID fragment ions correspond to y-type fragment ions, viz., fragment ions formed by cleavage of the amide bond with charge retention by the C-terminus.[73]

https://dx.doi.org/10.1021/acs.analchem.0c00829
Anal. Chem. 2020, 92, 8923−8932

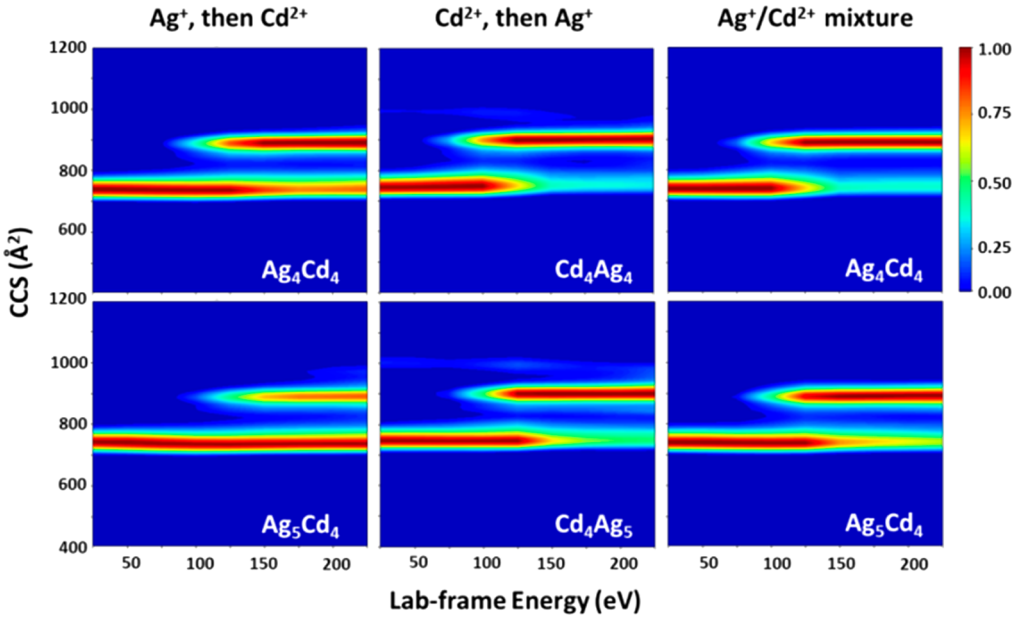

Figure 4. Collision-induced unfolding (CIU) heat maps for Ag_4Cd_4-MT, Ag_5Cd_4-MT, Cd_4Ag_4-MT, and Cd_4Ag_5-MT. The legends at the top of each panel provide the sequence of the addition of each metal ion.

Assignments for the CID fragment ions of the Ag_4NEM_{14}-MT species are in Figure 3D. A series of metal-free, α-domain CID fragments ranging from y2 to y29 also contain 1 to 11 NEM labeled residues and serve as evidence that none of the cysteine residues in the α-domain are involved in Ag^+ binding (see Figure 3D). In addition, Cys5 and Cys7 are also labeled by NEM, which indicates that these sites are not involved in binding Ag^+ or that the metal binding is weak relative to other binding sites. Among the 7 cysteine residues between Cys13 and Cys29, 6 are involved in binding Ag^+ ions and one is labeled by NEM. The limited fragment ion coverage from Ser12 to Ser32 does not allow identification among Cys13 to Cys29; however, similar results for the β-domain discussed below help to resolve this issue.

IM-MS data of tryptic digested Ag_4NEM_{14}-MT were used to assign the Ag^+ binding sites of the β-domain. Tryptic digestion of Ag_4NEM_{14}-MT produced a number of peptides corresponding to cleavages of the α-domain (see Figure S3 and Table S1) as well as tryptic fragments corresponding to the intact β-domain, viz., m/z 1329.62 (3+) (GlySer-Met1-Lys30) containing four Ag^+ ions and three NEM labels. The CIU heat map (Figure S4A) suggests that the Ag_4NEM_3-β-domain^{3+} is quite stable; viz., the complex does not unfold even at the highest CE, and the MS-CID-IM-MS data (Figure S4B,C) provide strong evidence that Cys5, Cys7, and Cys29 are bound to NEM and the four Ag^+ ions of the Ag_4NEM_3-β-domain are bound to Cys13, Cys15, Cys19, Cys21, Cys24. and Cys26.

Note that fragments from y3 to y9 contain one NEM and no Ag^+ ion, which suggests that, among Cys24, Cys26, and Cys29, only Cys29 is labeled by NEM. Cys24 and Cys26 are coordinated with Ag^+ ions, but the binding between these two cysteines and Ag^+ ions are relatively weak upon collisional activation. Lastly, missed tryptic cleavages at Lys20, Lys22, and Lys25 suggest that these residues are buried within a relatively stable Ag_4Cys_6 cluster, which is consistent with the CIU heat map (Figure S4A) for a high degree of stability of the Ag_4Cys_6 cluster.

The top-down/bottom-up proteomics analyses of the NEM labeled Ag_4-MT are interpreted as evidence that Ag^+ ions in this complex are located in the β-domain, specifically binding to Cys13, Cys15, Cys19, Cys21, Cys24, and Cys26. Palacios et al. previously reported that both Ag^+ and Cu^+ preferentially bind to the β-domain of MT to yield M_6-βMT.[19] Nielson and Winge,[74] Bofill et al.,[75] and Li and Otvos[76,77] also suggested that Ag^+ ions bind to the β-domain; however, Scheller et al. noted that "Experimentally, this was very hard to prove...".[20] The results of the NEM displacement reactions provide clear evidence that Ag^+ ions of Ag_4-MT are bound in the β-domain, but the absence of a similar product, Ag_6-MT, appears to contradict these previous assignments. An alternative explanation could be that two of the Ag^+ ions bound in the β-domain of Ag_6-MT are more weakly bound. We suggest that the weakly bound Ag^+ ions are possibly coordinated to Cys5, Cys7, and Cys29 and possibly bridging to Cys of the α-domain.

The assignment by Palacios et al. of a stable Ag-MT complex was based on results obtained from UV−vis absorption, CD spectroscopy, and MS during the stepwise replacement of Zn^{2+} by the addition of Ag^+ ions to solutions containing Zn_7-MT.[19] Using MS, they observed Ag_4Zn_5-MT and Ag_4Zn_1-βMT as the major product ions formed by the replacement of Zn by Zn_7-MT and Zn_3-βMT, respectively.[19] It is interesting to note that stable complexes with four Cu^+ ions have also been reported.[20,78] The integration of ESI-IM-MS, top-down and bottom-up proteomics with NEM labeling provides more definitive evidence regarding the Ag^+ ion binding sites and will be extended to the Cu^+ study.

Collision-Induced Unfolding (CIU) of Ag_i/Cd_i-MT and Ag_i-MT: Relative Stabilities of Metalated MT. Results of the NEM displacement studies raise questions about the relative Ag^+-MT binding energies, but it is difficult to obtain accurate metal ion binding energies. Previous studies have shown that the sequential addition of metal ions to MTs promote formation of more compact structures,[46] and collision-induced dissociation (CIU) can be used to gain insights into how metalation changes the stabilities of the MT

https://dx.doi.org/10.1021/acs.analchem.0c00829
Anal. Chem. 2020, 92, 8923−8932

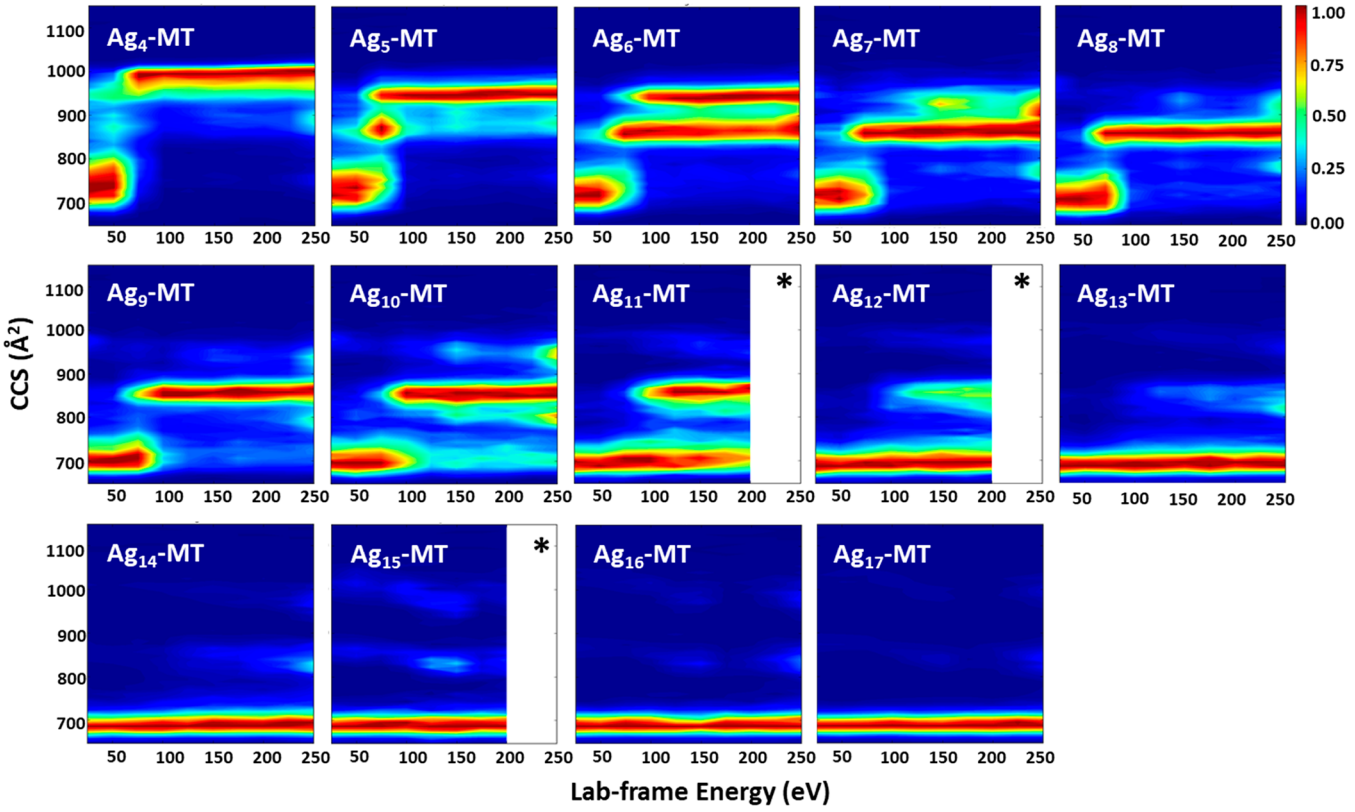

Figure 5. CIU heat maps for Ag_4-MT to Ag_{17}-MT. Asterisks (*) indicate that the CIU heat maps are truncated due to collision-induced dissociation. CID forms fragmentations from the N-terminus; no Ag^+ dissociation is detected.

complex. Figure 4 contains CIU heat maps for the mixed metal complexes, i.e., Ag_4Cd_4-MT, Ag_5Cd_4-MT, Cd_4Ag_4-MT, and Cd_4Ag_5-MT. Prior to collisional activation, the CCS profile for Ag_4Cd_4-MT ions is centered at ~750 Å^2; CCS profiles at different CEs are contained in Figure S5. A portion of the ions unfold at ~75 eV (E_{lab}) to around 900 Å^2, while the CCS for the remaining ions is unchanged. Similar results are observed for Cd_4Ag_4-MT, except that Cd_4Ag_4-MT unfolds at lower activation energy than Ag_4Cd_4-MT. The CCS profile for Ag_5Cd_4-MT ions is centered at ~750 Å^2, but a population of Ag_5Cd_4-MT ions unfolds at ~100 eV to around 900 Å^2, while the majority stays folded upon collisional activation. Similar results are observed for Cd_4Ag_5-MT, except that Cd_4Ag_5-MT unfolds at a lower activation energy than does Ag_5Cd_4-MT. Intriguingly, the addition of Cd^{2+} followed by the addition of Ag^+ and the addition of a Ag^+/Cd^{2+} mixture to apo-MT yield almost identical CIU heat maps, whereas the addition of Ag^+ followed by the addition of Cd^{2+} yields product ions that retain a higher abundance of the compact, folded conformers at all activation energies.

Note that the CIUs of Cd_4Ag_4- and Ag_4Cd_4-MT show some dependence on the order of metal addition. This effect is attributed to the influence of Cys33, which was previously shown to be highly solvent exposed, and a weak binding site of Cd^{2+} ions that can be displaced upon addition of NEM.[53,79] Cys33 may also have weak interactions with Ag^+ in the formation of Ag_4-MT. With the addition of Cd^{2+}, the interaction between Cys33 and Ag^+ can be partially maintained. However, if Cd^{2+} is added before Ag^+, the Cd_4Cys_{11} cluster formed in the α-domain may inhibit interactions between Ag^+ and Cys33. As a result, MT metalated by Ag^+ and then by Cd^{2+} produces a higher abundance of compact conformer than MT metalated by Cd^{2+} first or by the Ag^+/Cd^{2+} mixture.

CIU was also used to compare the gas-phase stabilities of the various Ag_i-MT (i = 4−17) complexes (Figure 5).[46,62] CCS profiles for the Ag_4-MT ions are relatively broad and span the range from ~650 to 800 Å^2, and low abundance signals are observed as high as 950 Å^2 (see Figure S6). Similar to that observed for apo-MT, the width of the CCS profile is a signature for a conformationally disordered ion population.[46] As the CE is increased, the CCS of the ions increase to a maximum value of ~1000 Å^2. For example, at a CE of ~45 eV, the abundances of ions with a CCS of 750 Å^2 decreased and those in the range from ~850 Å^2 steadily increased; at a CE of approximately 60 eV, the abundances of ions with CCS ~ 950 Å^2 increased, and at a CE of ~75 eV, conformers reached a maximum CCS of ~1000 Å^2.

Although the CCSs for Ag_5-MT to Ag_7-MT show some differences, an intermediate state is observed across a narrow range of CE for Ag_5-MT. A similar state is observed for Ag_6- and Ag_7-MT, but this state appears to be more stable than that observed for Ag_5-MT. In fact, a state with a similar CCS (~875 Å^2) appears to be the final state for Ag_8-, Ag_9-, Ag_{10}-, and Ag_{11}-MT.

The CIU heat maps for Ag_4-MT through Ag_7-MT show considerable differences, whereas those for Ag_8-MT through Ag_{11}-MT are quite similar. At a low CE, the CCSs of Ag_8- to Ag_{11}-MT center on ~700 Å^2 and a maximum value ~850 Å^2 at the higher CEs; however, the threshold CE required to produce ions having the higher CCS increases as the number of bound Ag^+ ions increases from a CE value of ~55 eV for Ag_4-MT to ~110 eV for Ag_{11}-MT. For Ag_{12}-MT through Ag_{17}-MT, the CCS remains constant; for all of these ions, no change

https://dx.doi.org/10.1021/acs.analchem.0c00829
Anal. Chem. 2020, 92, 8923−8932

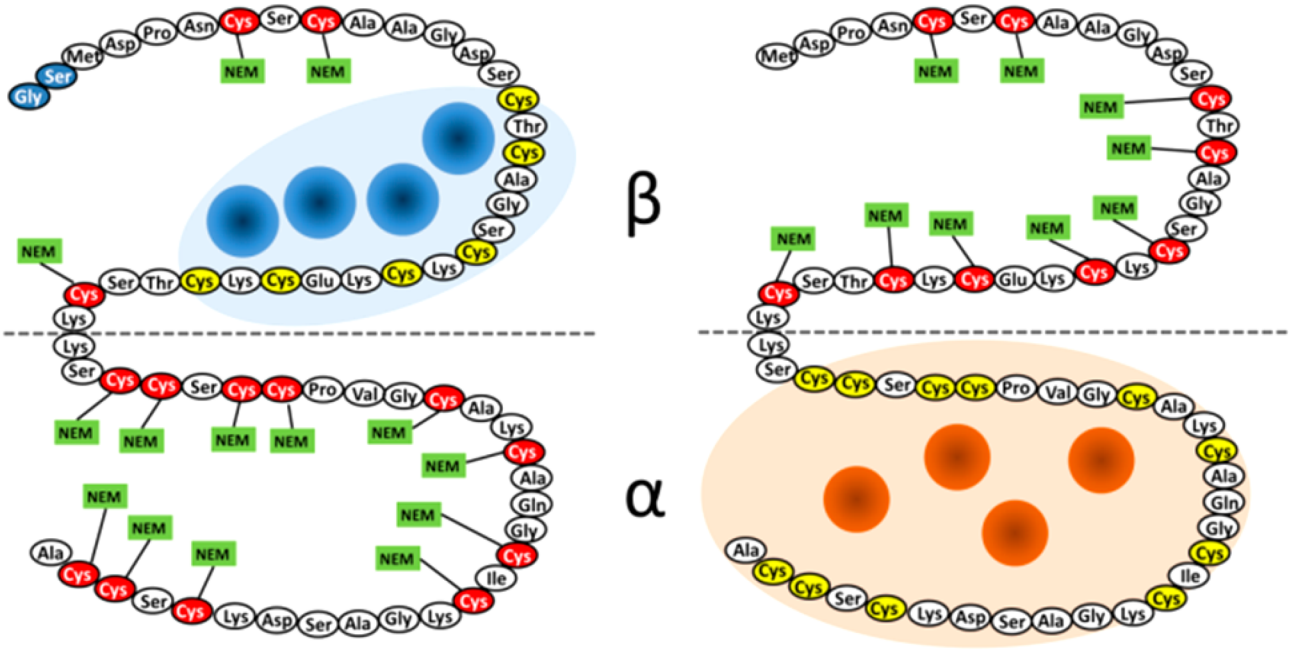

Figure 6. Summary of binding sites identification. Ag^+ ions (blue) of Ag_4-MT are located in the β-domain, whereas Cd^{2+} ions (orange) of Cd_4-MT are located in the α-domain. The binding sites for Cd_4-MT are summarized from a previous publication.[45]

in CCS occurs as CE is increased. However, at high energies (200 eV), some of these ions begin to dissociate, without loss of Ag^+ ions.

There is a sharp drop in the CCSs for Ag_{12}-MT through Ag_{17}-MT. Zelazowski et al.,[21] Nielson and Winge,[74] and Li and Otvos[76] have shown that apo-MT requires at least 12 Ag^+ ions to fully metalate both domains, which is also supported by the results reported here. Ag_{12}-MT is resistant to unfolding because both domains are fully metalated. Ag^+ can adopt two different binding geometries with thiolates: trigonal and digonal.[1,17] For trigonal binding geometries, each Ag^+ ion interacts with three cysteines, whereas in digonal binding geometries, each Ag^+ ion interacts with two cysteines. The details of silver coordination are still open to debate. The only Ag^+ metalated MT structure reported in the Protein Data Bank database for *Saccharomyces cerevisiae* was obtained by NMR. It appears that this system adopts a mixed coordination number of 2 and 3 for the seven bound Ag^+ ions. Gui et al. investigated metal coordination of Ag_{12}-MT and Ag_{17}-MT from rabbit liver using K-edge X-ray absorption spectroscopy (XAS) and concluded that the Ag^+ ions in both Ag_{12}-MT and Ag_{17}-MT are digonally coordinated by thiolates; the difference is that there are more bridging sulfurs in Ag_{17}-MT than in Ag_{12}-MT.[24] More recent work also using XAS by Veronesi et al. showed that Ag^+ occupies trigonal sites mainly (~70%) for the same isoform.[25] Both geometry changes of Ag^+ and the fraction change of bridging and terminal sulfur may lead to the formation of Ag_{17}-MT from Ag_{12}-MT. The CCS profiles for Ag_i-MT (i = 4−17) under different activation energies are summarized in Figure S7.

Another possible mechanism for the formation of Ag_{12}- to Ag_{17}-MT is the influence of Ag−Ag interaction.[80,81] That is, the formation of Ag nanoclusters has been previously reported for nucleic acids/silver complexes,[82−84] and similar products may be formed by partially and/or fully metalated MTs. Studies are underway to explore whether silver nanoclusters are indeed formed in our ESI-MS experiments.

For comparison, ESI-MS spectra and CIU heat maps for Ag_i-rMT (rabbit MT) are provided as Figures S8 and S9, respectively. The CCSs for Ag_i-rMT are somewhat larger than those for Ag_i-MT, but CIU heat maps for Ag_i-rMT and Ag_i-MT show similar changes. Blindauer and Leszczyszyn state that the folding of MTs is dominated by metal binding and the formation of metal−cysteine clusters;[1] therefore, the structure should be mainly influenced by metal ions and cysteine residuals involved in metal binding. In our experiment, CIU heat maps during Ag^+ titration are quite similar for both types of MTs, which indicates similar stabilities of Ag_i-rMT and Ag_i-MT (i = 4−17). This is consistent with Blindauer and Leszczyszyn's statement.

CONCLUSIONS

The comprehensive ESI-IM-MS approach employed here provides new insights about the metalation of human metallothionein-2A, both in terms of the metal ion binding sites and the relative stabilities of the Ag_i-MT complexes. Results from these studies provide clear evidence that Ag^+ ions of the Ag_4-MT complex are bound in the β-domain. Bottom-up and top-down proteomics experiments clearly show that the Ag^+ ions are bound to Cys13, Cys15, Cys19, Cys21, Cys24, and Cys26, a binding arrangement that is very different from that of Cd^{2+}; viz., the Cd^{2+} ions that react to form Cd_4-MT are located in the α-domain.[45] This is also supported by results from studies with mixed metal ions (Ag^+/Cd^{2+}). However, results from collision-induced dissociation show that the unfolding process of Ag_4Cd_4-MT, Cd_4Ag_4-MT, Ag_5Cd_4-MT, and Cd_4Ag_5-MT is similar but not identical. The difference in unfolding may originate from some (see Figure 6) intramolecular interactions between the two domains with dependency on the order of metal ion addition. Overall, the combination of MS and IM (CIU) provides a comprehensive understanding of the relationship between α- and β-domains. The different metal ion binding for these divalent and monovalent metal ions may be important in heavy metal

https://dx.doi.org/10.1021/acs.analchem.0c00829
Anal. Chem. 2020, 92, 8923−8932

detoxification and homeostasis involving different metal species.

Higher order Ag_i-MT clusters (i = 5−17) are formed when excess Ag^+ is added to solutions containing MT. Upon addition of *N*-ethylmalemide (NEM) to this solution, metal displacement produces Ag_4NEM_{14}-MT as the major product (>90%). This result is consistent with our assignment of higher binding energies of the four Ag^+ ions located in the β-domain. Previous studies have reported compelling evidence for the formation of a Ag_6-MT, and it was suggested that all six Ag^+ ions are bound in the β-domain.[19,74,76,77] Although we do not detect Ag_6NEM_i-MT complexes, we do feel that this observation contradicts the prior assignment of a stable Ag_6 cluster for Ag_6-MT. Instead, we suggest that in forming Ag_6 clusters, two Ag^+ ions are more weakly bound compared to the Ag^+ ions that bind to Cys13, Cys15, Cys19, Cys21, Cys24, and Cys26.

Ag^+ ions of Ag_i-MT (i = 5 to 14) can be displaced by NEM to form Ag_4NEM_{14}-MT. Such metal displacement was reported previously.[53,72] In those cases, the dissociation equilibrium of the metal−thiolate bond provides thiolate sites that are weakly associated with metal ions; those thiolate sites are reactive with NEM.[53,72] The Ag^+ ions that can be replaced by NEM are more labile in the solution phase.

■ ASSOCIATED CONTENT

Supporting Information

The Supporting Information is available free of charge at https://pubs.acs.org/doi/10.1021/acs.analchem.0c00829.

Experimental procedures for MT expression and purification, MT demetalation, and bottom-up proteomics; detailed MS spectra for apo-MT, Ag_9- to Ag_{14}-MT, and Ag_4NEM_{14}-MT; isotopic distribution of Ag_4-MT and Cd_4-MT and the overlap peaks of Ag_4- and Cd_4-MT and Ag_2Cd_2-MT; MS spectra and identified fragment ions of Ag_4NEM_{14}-MT after tryptic digestion; CCS profiles for 5+ ions of Ag_4Cd_4-, Ag_5Cd_4-, Cd_4Ag_4-, and Cd_4Ag_5-MT under different collisional activation conditions; CCS profiles for 5+ ions of apo- and Ag_i-MT (i = 4−17); CCS change of Ag_i-MT (i = 4−17) during Ag^+ titration; ESI-MS spectra and CIU of rabbit MT; identified fragmentation ions (PDF)

■ AUTHOR INFORMATION

Corresponding Author

David H. Russell − *Department of Chemistry, Texas A&M University, College Station, Texas 77843, United States;* orcid.org/0000-0003-0830-3914; Email: russell@chem.tamu.edu

Authors

Shiyu Dong − *Department of Chemistry, Texas A&M University, College Station, Texas 77843, United States*

Mehdi Shirzadeh − *Department of Chemistry, Texas A&M University, College Station, Texas 77843, United States*

Liqi Fan − *Department of Chemistry, Texas A&M University, College Station, Texas 77843, United States*

Arthur Laganowsky − *Department of Chemistry, Texas A&M University, College Station, Texas 77843, United States;* orcid.org/0000-0001-5012-5547

Complete contact information is available at: https://pubs.acs.org/10.1021/acs.analchem.0c00829

Notes

The authors declare no competing financial interest.

■ ACKNOWLEDGMENTS

This work was supported by the National Institutes of Health (R01GM121751 and P41GM128577), the National Science Foundation (CHE-1707675), and endowment funds provided by the MDS Sciex Professorship.

■ REFERENCES

(1) Blindauer, C. A.; Leszczyszyn, O. I. *Nat. Prod. Rep.* **2010**, *27* (5), 720−741.
(2) Capdevila, M.; Bofill, R.; Palacios, O.; Atrian, S. *Coord. Chem. Rev.* **2012**, *256* (1−2), 46−62.
(3) Scheller, J. S.; Irvine, G. W.; Stillman, M. J. *Dalton T* **2018**, *47* (11), 3613−3637.
(4) Vallee, B. L. *Neurochem. Int.* **1995**, *27* (1), 23−33.
(5) Coyle, P.; Philcox, J. C.; Carey, L. C.; Rofe, A. M. *Cell. Mol. Life Sci.* **2002**, *59* (4), 627−647.
(6) Davis, S. R.; Cousins, R. J. *J. Nutr.* **2000**, *130* (5), 1085−1088.
(7) Kang, Y. J. *Exp. Biol. Med.* **2006**, *231* (9), 1459−1467.
(8) Lu, W. H.; Zelazowski, A. J.; Stillman, M. J. *Inorg. Chem.* **1993**, *32* (6), 919−926.
(9) Yang, Y.; Maret, W.; Vallee, B. L. *Proc. Natl. Acad. Sci. U. S. A.* **2001**, *98* (10), 5556−5559.
(10) Giles, N. M.; Watts, A. B.; Giles, G. I.; Fry, F. H.; Littlechild, J. A.; Jacob, C. *Chem. Biol.* **2003**, *10* (8), 677−693.
(11) Bell, S. G.; Vallee, B. L. *ChemBioChem* **2009**, *10* (1), 55−62.
(12) Petering, D. H.; Mahim, A. *Int. J. Mol. Sci.* **2017**, *18* (6), 1289.
(13) Arseniev, A.; Schultze, P.; Worgotter, E.; Braun, W.; Wagner, G.; Vasak, M.; Kagi, J. H. R.; Wuthrich, K. *J. Mol. Biol.* **1988**, *201* (3), 637−657.
(14) Narula, S. S.; Mehra, R. K.; Winge, D. R.; Armitage, I. M. *J. Am. Chem. Soc.* **1991**, *113* (24), 9354−9358.
(15) Blindauer, C. A.; Harrison, M. D.; Parkinson, J. A.; Robinson, A. K.; Cavet, J. S.; Robinson, N. J.; Sadler, P. J. *Proc. Natl. Acad. Sci. U. S. A.* **2001**, *98* (17), 9593−9598.
(16) Peroza, E. A.; Schmucki, R.; Guntert, P.; Freisinger, E.; Zerbe, O. *J. Mol. Biol.* **2009**, *387* (1), 207−218.
(17) Peterson, C. W.; Narula, S. S.; Armitage, I. M. *FEBS Lett.* **1996**, *379* (1), 85−93.
(18) Calderone, V.; Dolderer, B.; Hartmann, H. J.; Echner, H.; Luchinat, C.; Del Bianco, C.; Mangani, S.; Weser, U. *Proc. Natl. Acad. Sci. U. S. A.* **2005**, *102* (1), 51−56.
(19) Palacios, O.; Polec-Pawlak, K.; Lobinski, R.; Capdevila, M.; Gonzalez-Duarte, P. *JBIC, J. Biol. Inorg. Chem.* **2003**, *8* (8), 831−842.
(20) Scheller, J. S.; Irvine, G. W.; Wong, D. L.; Hartwig, A.; Stillman, M. J. *Metallomics* **2017**, *9* (5), 447−462.
(21) Zelazowski, A. J.; Gasyna, Z.; Stillman, M. J. *J. Biol. Chem.* **1989**, *264* (29), 17091−17099.
(22) Scheuhammer, A. M.; Cherian, M. G. *Toxicol. Appl. Pharmacol.* **1986**, *82* (3), 417−425.
(23) Bertini, I.; Hartmann, H. J.; Klein, T.; Liu, G. H.; Luchinat, C.; Weser, U. *Eur. J. Biochem.* **2000**, *267* (4), 1008−1018.
(24) Gui, Z.; Green, A. R.; Kasrai, M.; Bancroft, G. M.; Stillman, M. J. *Inorg. Chem.* **1996**, *35* (22), 6520−6529.
(25) Veronesi, G.; Gallon, T.; Deniaud, A.; Boff, B.; Gateau, C.; Lebrun, C.; Vidaud, C.; Rollin-Genetet, F.; Carriere, M.; Kieffer, I.; Mintz, E.; Delangle, P.; Michaud-Soret, I. *Inorg. Chem.* **2015**, *54* (24), 11688−11696.
(26) Yu, X. L.; Wojciechowski, M.; Fenselau, C. *Anal. Chem.* **1993**, *65* (10), 1355−1359.
(27) Fabris, D.; Zaia, J.; Hathout, Y.; Fenselau, C. *J. Am. Chem. Soc.* **1996**, *118* (48), 12242−12243.
(28) Kagi, J. H. R.; Vallee, B. L. *J. Biol. Chem.* **1960**, *235* (12), 3460−3465.
(29) Messerle, B. A.; Schaffer, A.; Vasak, M.; Kagi, J. H. R.; Wuthrich, K. *J. Mol. Biol.* **1990**, *214* (3), 765−779.

(30) Messerle, B. A.; Schaffer, A.; Vasak, M.; Kagi, J. H. R.; Wuthrich, K. *J. Mol. Biol.* **1992**, *225* (2), 433−443.
(31) Gehrig, P. M.; You, C. H.; Dallinger, R.; Gruber, C.; Brouwer, M.; Kagi, J. H. R.; Hunziker, P. E. *Protein Sci.* **2000**, *9* (2), 395−402.
(32) Chassaigne, H.; Lobinski, R. *J. Chromatogr A* **1998**, *829* (1−2), 127−136.
(33) Chassaigne, H.; Lobinski, R. *Analyst* **1998**, *123* (10), 2125−2130.
(34) Mounicou, S.; Polec, K.; Chassaigne, H.; Potin-Gautier, M.; Lobinski, R. *J. Anal. At. Spectrom.* **2000**, *15* (6), 635−642.
(35) Domenech, J.; Orihuela, R.; Mir, G.; Molinas, M.; Atrian, S.; Capdevila, M. *JBIC, J. Biol. Inorg. Chem.* **2007**, *12* (6), 867−882.
(36) Orihuela, R.; Domenech, J.; Bofill, R.; You, C.; Mackay, E. A.; Kagi, J. H. R.; Capdevila, M.; Atrian, S. *JBIC, J. Biol. Inorg. Chem.* **2008**, *13* (5), 801−812.
(37) Domenech, J.; Bofill, R.; Tinti, A.; Torreggiani, A.; Atrian, S.; Capdevila, M. *Biochim. Biophys. Acta, Proteins Proteomics* **2008**, *1784* (4), 693−704.
(38) Palacios, O.; Espart, A.; Espin, J.; Ding, C.; Thiele, D. J.; Atrian, S.; Capdevila, M. *Metallomics* **2014**, *6* (2), 279−291.
(39) Ngu, T. T.; Stillman, M. J. *J. Am. Chem. Soc.* **2006**, *128* (38), 12473−12483.
(40) Ngu, T. T.; Easton, A.; Stillman, M. J. *J. Am. Chem. Soc.* **2008**, *130* (50), 17016−17028.
(41) Sutherland, D. E. K.; Willans, M. J.; Stillman, M. J. *J. Am. Chem. Soc.* **2012**, *134* (6), 3290−3299.
(42) Mierek-Adamska, A.; Dabrowska, G. B.; Blindauer, C. A. *Metallomics* **2018**, *10* (10), 1430−1443.
(43) Imam, H. T.; Blindauer, C. A. *JBIC, J. Biol. Inorg. Chem.* **2018**, *23* (1), 137−154.
(44) M'kandawire, E.; Mierek-Adamska, A.; Sturzenbaum, S. R.; Choongo, K.; Yabe, J.; Mwase, M.; Saasa, N.; Blindauer, C. A. *Int. J. Mol. Sci.* **2017**, *18* (7), 1548.
(45) Chen, S. H.; Russell, W. K.; Russell, D. H. *Anal. Chem.* **2013**, *85* (6), 3229−3237.
(46) Dong, S. Y.; Wagner, N. D.; Russell, D. H. *Anal. Chem.* **2018**, *90* (20), 11856−11862.
(47) Patrick, J. W.; Gamez, R. C.; Russell, D. H. *Anal. Chem.* **2015**, *87* (1), 578−583.
(48) Hopper, J. T. S.; Oldham, N. J. *J. Am. Soc. Mass Spectrom.* **2009**, *20* (10), 1851−1858.
(49) Laganowsky, A.; Reading, E.; Allison, T. M.; Ulmschneider, M. B.; Degiacomi, M. T.; Baldwin, A. J.; Robinson, C. V. *Nature* **2014**, *510* (7503), 172−175.
(50) Wagner, N. D.; Kim, D.; Russell, D. H. *Anal. Chem.* **2016**, *88* (11), 5934−5940.
(51) Chen, S. H.; Chen, L. X.; Russell, D. H. *J. Am. Chem. Soc.* **2014**, *136* (26), 9499−9508.
(52) Chen, S. H.; Russell, D. H. *J. Am. Soc. Mass Spectrom.* **2015**, *26* (9), 1433−1443.
(53) Chen, S. H.; Russell, D. H. *Biochemistry* **2015**, *54* (39), 6021−6028.
(54) Wagner, N. D.; Russell, D. H. *J. Am. Chem. Soc.* **2016**, *138* (51), 16588−16591.
(55) Hogstrand, C.; Galvez, F.; Wood, C. M. *Environ. Toxicol. Chem.* **1996**, *15* (7), 1102−1108.
(56) Osobova, M.; Urban, V.; Jedelsky, P. L.; Borovicka, J.; Gryndler, M.; Ruml, T.; Kotrba, P. *New Phytol.* **2011**, *190* (4), 916−926.
(57) Han, L. J.; Hyung, S. J.; Mayers, J. J. S.; Ruotolo, B. T. *J. Am. Chem. Soc.* **2011**, *133* (29), 11358−11367.
(58) Tian, Y. W.; Han, L. J.; Buckner, A. C.; Ruotolo, B. T. *Anal. Chem.* **2015**, *87* (22), 11509−11515.
(59) Watanabe, Y.; Vasiljevic, S.; Allen, J. D.; Seabright, G. E.; Duyvesteyn, H. M. E.; Doores, K. J.; Crispin, M.; Struwe, W. B. *Anal. Chem.* **2018**, *90* (12), 7325−7331.
(60) Tian, Y. W.; Ruotolo, B. T. *Int. J. Mass Spectrom.* **2018**, *425*, 1−9.
(61) Tian, Y. W.; Ruotolo, B. T. *Analyst* **2018**, *143* (11), 2459−2468.
(62) Dixit, S. M.; Polasky, D. A.; Ruotolo, B. T. *Curr. Opin. Chem. Biol.* **2018**, *42*, 93−100.
(63) Zinnel, N. F.; Pai, P. J.; Russell, D. H. *Anal. Chem.* **2012**, *84* (7), 3390−3397.
(64) Zinnel, N. F.; Russell, D. H. *Anal. Chem.* **2014**, *86* (10), 4791−4798.
(65) McLean, J. A.; Ruotolo, B. T.; Gillig, K. J.; Russell, D. H. *Int. J. Mass Spectrom.* **2005**, *240* (3), 301−315.
(66) Eschweiler, J. D.; Rabuck-Gibbons, J. N.; Tian, Y. W.; Ruotolo, B. T. *Anal. Chem.* **2015**, *87* (22), 11516−11522.
(67) Polasky, D. A.; Dixit, S. M.; Fantin, S. M.; Ruotolo, B. T. *Anal. Chem.* **2019**, *91* (4), 3147−3155.
(68) Testa, L.; Brocca, S.; Grandori, R. *Anal. Chem.* **2011**, *83* (17), 6459−6463.
(69) Grabenauer, M.; Wyttenbach, T.; Sanghera, N.; Slade, S. E.; Pinheiro, T. J. T.; Scrivens, J. H.; Bowers, M. T. *J. Am. Chem. Soc.* **2010**, *132* (26), 8816−8818.
(70) Pai, P. J.; Cologna, S. M.; Russell, W. K.; Vigh, G.; Russell, D. H. *Anal. Chem.* **2011**, *83* (7), 2814−2818.
(71) Salgado, M. T.; Bacher, K. L.; Stillman, M. J. *JBIC, J. Biol. Inorg. Chem.* **2007**, *12* (3), 294−312.
(72) Shaw, C. F.; He, L. B.; Munoz, A.; Savas, M. M.; Chi, S.; Fink, C. L.; Gan, T.; Petering, D. H. *JBIC, J. Biol. Inorg. Chem.* **1997**, *2* (1), 65−73.
(73) Roepstorff, P.; Fohlman, J. *Biomed. Mass Spectrom.* **1984**, *11* (11), 601−601.
(74) Nielson, K. B.; Winge, D. R. *J. Biol. Chem.* **1985**, *260* (15), 8698−8701.
(75) Bofill, R.; Palacios, O.; Capdevila, M.; Cols, N.; Gonzalez-Duarte, R.; Atrian, S.; Gonzalez-Duarte, P. *J. Inorg. Biochem.* **1999**, *73* (1−2), 57−64.
(76) Li, H.; Otvos, J. D. *Biochemistry* **1996**, *35* (44), 13929−13936.
(77) Li, H.; Otvos, J. D. *J. Inorg. Biochem.* **1998**, *70* (3−4), 187−194.
(78) Jensen, L. T.; Peltier, J. M.; Winge, D. R. *JBIC, J. Biol. Inorg. Chem.* **1998**, *3* (6), 627−631.
(79) Robbins, A. H.; Mcree, D. E.; Williamson, M.; Collett, S. A.; Xuong, N. H.; Furey, W. F.; Wang, B. C.; Stout, C. D. *J. Mol. Biol.* **1991**, *221* (4), 1269−1293.
(80) Hu, S. Q.; Ye, B. Y.; Yi, X. Y.; Cao, Z. Z.; Wu, D. H.; Shen, C. C.; Wang, J. X. *Talanta* **2016**, *155*, 272−277.
(81) Cui, Y. Y.; Wang, Y. L.; Zhao, L. N. *Small* **2015**, *11* (38), 5118−5125.
(82) Choi, S.; Yu, J. H. *APL Mater.* **2017**, *5* (5), 053401.
(83) Sych, T. S.; Reveguk, Z. V.; Pomogaev, V. A.; Buglak, A. A.; Reveguk, A. A.; Ramazanov, R. R.; Romanov, N. M.; Chikhirzhina, E. V.; Polyanichko, A. M.; Kononov, A. I. *J. Phys. Chem. C* **2018**, *122* (51), 29549−29558.
(84) Huard, D. J. E.; Demissie, A.; Kim, D.; Lewis, D.; Dickson, R. M.; Petty, J. T.; Lieberman, R. L. *J. Am. Chem. Soc.* **2019**, *141*, 11465.

https://dx.doi.org/10.1021/acs.analchem.0c00829
Anal. Chem. 2020, 92, 8923−8932